Quasioptical Reflective Polarization Modulation for the Beyond Einstein Inflation Probe

David T. Chuss
NASA Goddard Space Flight Center, Code 665, Greenbelt, MD 20771
E-mail: David.T.Chuss@nasa.gov

Abstract. Polarization modulators that are based on the introduction of a quasioptical phase delay between two orthogonal linear polarizations are reviewed. The general principle behind the device and the application to the Beyond Einstein Inflation Probe are addressed.

1. Introduction

Polarization modulation allows for clean separation of the polarized light from a source and the unpolarized background. This is likely to be an important element in systems designed to search for the B-mode polarization as the unpolarized contribution from the Cosmic Microwave Background (CMB) is much larger than the faint signature of inflation.

It is desirable that a polarization modulator not change the total coherence of the signal that it is modulating. That is, for polarization modulation having low systematics, it is advantageous, and perhaps required, that the total polarization ($P^2 = Q^2 + U^2 + V^2$) remain the same throughout the modulation process. This corresponds to a path on the Poincaré sphere. Such an operation can be physically produced by introducing a phase delay between two orthogonal polarization states.

Though there are various ways to do this in practice, this white paper will explore techniques that do this quasioptically and in reflection by adding a phase delay between orthogonal *linear* polarizations. This is most commonly done using a system of polarizers and mirrors. Specifically, it will focus on the Variable-delay Polarization Modulator (VPM). This device modulates the phase between two orthogonal linear polarizations by changing the separation between a grid and mirror. A major advantage of this device is that it can be constructed large enough to be used as the first element in the optical system thereby avoiding most of the instrumental polarization of the system. It can also modulate polarization on time scales (∼few Hz) that will allow the 1/f mitigation to be done in polarization rather than in a spatial scanning mode. This combination of front-end placement and modulation in polarization is a potential advantage of the VPM since it avoids systematics that mix unpolarized anisotropy into a false polarization signal. Calibration techniques associated with such an architecture may be especially suited to polarimetry at large angular scales in which scanning calibration schemes are problematic. In addition, the symmetry of the polarization separation in the VPM can be exploited to provide additional systematic controls.

2. Heritage

This concept has heritage in the Martin Puplett interferometer (hereafter MPI) [1] which utilizes a variable phase introduction between two orthogonal linear polarizations to generate an interferogram that, when Fourier transformed, gives spectra of Stokes Q and V. The most common use of this device is as a spectrometer. In such an application, Stokes I of the input signal is mapped to Stokes Q using a polarizing grid (and Stokes V is set to zero) such as in the case of COBE/FIRAS [2]. Even so, the utility of an MPI as a polarization modulator was recognized in early works on the subject [3]. An MPI has been used in the MITOpol CMB spectropolarimeter [4, 5] in combination with a rotating Fresnel double rhomb for the purpose of characterizing the polarization spectrum of the CMB.

A more compact way of introducing a phase delay between two orthogonal polarizations is by placing a polarizing grid in front of and parallel to a mirror. The phase delay is then a function of the mirror-grid separation. Various implementations of this architecture exist in the literature. Howard [6] implements such a system as a polarization transforming reflector (PTR) operating at 1.05 mm. Such setups are common in microwave and radio applications for transforming polarization states. Houde [7] models a similar device (called a "reflecting polarizer" for an OVRO receiver that is used to transform the linear polarization from dust emission into circular polarization that is cross-corellated in the receiver [8]. A similar quarter-wave transformer was also used earlier by Erickson [9] for work at 0.9 mm.

A similar grid-mirror system has been employed by Manabe[10]. In this work, two such systems (here dubbed a "frequency-selective polarizer" or FSP) are used as an alternative to an MPI for interferometry. These authors find that such a system has more alignment tolerance than the MPI, but also introduces an added complexity of treating resonances in the grid-mirror cavity.

Erickson[11] has used a variant called a "Reflecting Polarizing Interferometer" (RPI) in which the grid-mirror cavity is filled with a dielectric. In this work, the RPI is tested as a filter element as an alternative to a Fabry-Perot interferometer.

Polarization modulation with grid-mirror devices has also been done. For such applications, it is possible to modulate polarization in one of two ways. First, one can vary the grid-mirror separation such as is done in the interferometric applications. Second, it is possible to use the device as a half- or quarter- wave plate by fixing the grid-mirror separation (usually to $\lambda/2$ or $\lambda/4$) and rotating the device. The former has been demonstrated in the submillimeter by Krejny[12] in which two VPMs are used to navigate the Poincaré sphere [13]. The Cosmic Foreground Explorer (COFE) used this type of modulation in an early configuration [14], but later moved to a spinning reflective-half wave plate (HWP) modulation [15]. Shinnaga[16] and Siringo[17] have also used the spinning reflective half-wave plate in the submillimeter.

The remainder of this white paper will focus on polarization modulation devices using the parallel grid-mirror system.

3. Operational Principle

The basic architecture that all of the grid-mirror systems discussed in the Introduction is shown in Figure 1. Radiation of an arbitrary polarization state is incident on the grid-mirror structure. The component of the light that is linearly polarized parallel to the grid wires reflects off of the grid. The orthogonal component gets transmitted by the grid, is reflected by the mirror and then passes through the grid again. The two beams recombine with a phase that is related to the path length. The path length in turn is a function of the incident angle and the grid-mirror separation.

$$l = 2d\cos\phi \tag{1}$$

This path difference gives a geometric phase delay of

$$\Delta = \frac{2\pi l}{\lambda} = \frac{4\pi d \cos\phi}{\lambda} \tag{2}$$

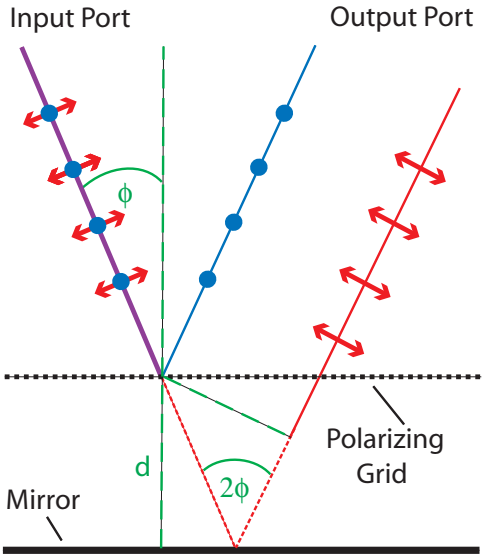

Figure 1. A phase delay between two orthogonal linear polarizations is introduced by an architecture in which a polarizing grid and a mirror are placed parallel to one another. The dotted red line indicates the physical path difference between the two polarizations.

Assuming that the wires are perfect polarizers and the grid wires are oriented at an angle θ with respect to the coordinate system of interest, the Mueller matrix for this system is

$$\begin{pmatrix} 1 & 0 & 0 & 0 \\ 0 & \cos^2 2\theta + \cos\Delta \sin^2 2\theta & -\sin 2\theta \cos 2\theta(1-\cos\Delta) & \sin 2\theta \sin\Delta \\ 0 & \sin 2\theta \cos 2\theta(1-\cos\Delta) & -\sin^2 2\theta - \cos\Delta \cos^2 2\theta & -\cos 2\theta \sin\Delta \\ 0 & \sin 2\theta \sin\Delta & \cos 2\theta \sin\Delta & -\cos\Delta \end{pmatrix} \tag{3}$$

For the case of the VPM, the angle is held fixed and the phase is modulated. Setting $\theta = 45°$ gives

$$\begin{pmatrix} 1 & 0 & 0 & 0 \\ 0 & \cos\Delta & 0 & \sin\Delta \\ 0 & 0 & -1 & 0 \\ 0 & \sin\Delta & 0 & -\cos\Delta \end{pmatrix}. \tag{4}$$

This operation is a combination of an inversion operation and rotation about the U-axis on the Poincaré sphere. Because of this, Stokes U is unmodulated, so full linear polarization measurement requires an additional step. Since Δ is dependent on wavelength, the modulation will become less coherent at higher orders, forming an interferogram that contains information about the polarization spectrum.

Conversely, for the reflective HWP, $\Delta = \pi$ and is fixed. The general matrix reduces to

$$\begin{pmatrix} 1 & 0 & 0 & 0 \\ 0 & \cos 4\theta & -\sin 4\theta & 0 \\ 0 & \sin 4\theta & \cos 4\theta & 0 \\ 0 & 0 & 0 & 1 \end{pmatrix} \tag{5}$$

which is recognizable as the Mueller matrix representing a HWP. Note that the path on the Poincaré sphere in this case is a circle in the Q-U plane. Here, linear polarization is completely modulated. Bandwidth effects dilute the signal in a direction perpendicular to the path in the Q-U plane, so the efficiency of the ideal reflective HWP is constant over the modulation, but falls off with increasing bandwidth. This architecture is tunable to multiple bands by changing the grid-mirror separation.

4. Current State-of-the-Art

Krejny [12] has reported astronomical use of a dual VPM system at 350 μm. For these observations, the VPM settings were not optimized, resulting in poor modulation efficiency. Nonetheless, an instrumental polarization of less than 1% was measured. Laboratory tests of a single VPM in this system are shown in Figure 2. In this figure, the data points represent the modulated signal as the grid-mirror separation was varied. The curve represents the polarization transfer function anticipated given the geometrical phase lag (Equation 2.) This has been adjusted in phase and amplitude to match the first peak for illustrative purposes. The difference in the observed phase as compared with that anticipated from the geometrical relationship is most likely due to the fact that the grid wires in this system are a measurable fraction of the wavelength (25 μm vs. 350 μm). This results in a phase shift contribution that is due the reactance of the system. This issue can be resolved by working in a regime where the wires are much smaller than the wavelength. The same VPM has been measured in a 3.15 mm system [18] and this effect was not observed (see the right side of Figure 2). In this plot, the solid line is the polarization transfer function based on the geometric phase delay between the two polarizations.

The polarization modulation efficiency is $\sim$80% for the 350 μm case, but is significantly higher at longer wavelengths. Part of this difference is due to the non-ideal efficiency of the VPM grid at 350 μm. The remainder is most likely due to differences in the optical systems in the two measurements.

This phase-separation relationship needs to be further quantified, especially in the application of VPMs to spectropolarimetry. The wire size, or perhaps more generally the set of polarizer parameters, is a key design consideration in constructing and implementing VPMs.

5. VPMs and CMB Polarization

The systematics of a VPM systematics as they apply to CMB polarimetry are highly-coupled to the instrument architecture in which the VPM is employed, so such a concept is briefly described here. We note as an aside that this differs from the Hertz/VPM implementation mentioned in the preceding section.

Figure 3 shows an optics concept for which the VPM is suited. In this case, the symmetry of the VPM is utilized. The VPM is the first element in the optical path in order to minimize instrumental polarization. This concept requires an array of polarized detectors with the direction of polarization sensitivity oriented at a 45° angle with respect to the wires of the VPM. For the ideal case, this system is described by expression 4. To first order, this system is insensitive to Stokes U, and thus requires an additional parameter (such as spacecraft or instrument rotation) to fully map the linear polarization. However, to counter this disadvantage, this system allows many of the systematic effects to be hidden in Stokes U without affecting the measurements of Stokes Q.

6. Systematic Effects

In many ways, the advantages and disadvantages of reflective HWP are similar to dielectric HWPs, so the following discussion of systematics will focus on the VPM configuration. However,

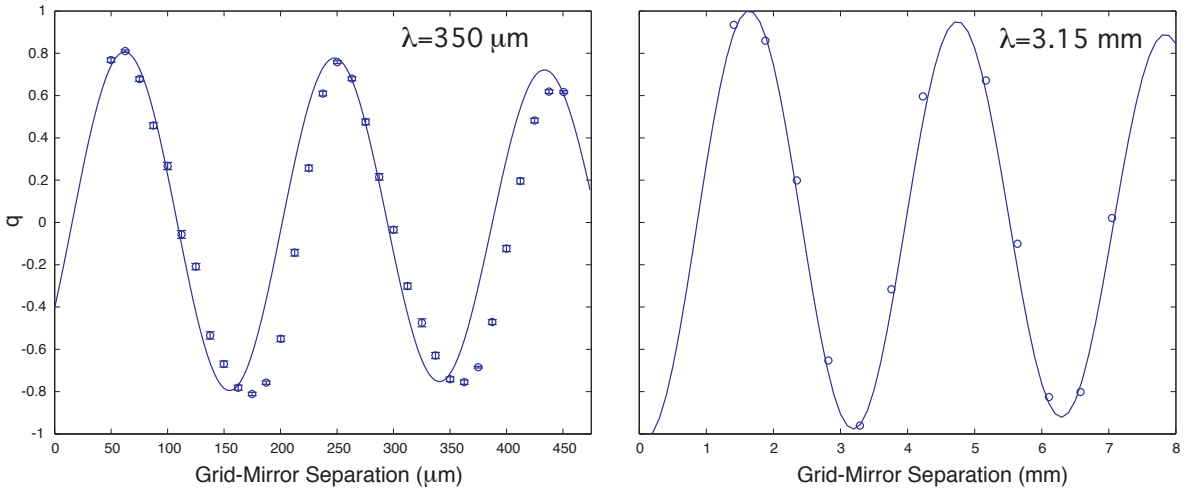

Figure 2. (left) The Hertz/VPM (350 μm) laboratory data is shown [12]. The solid line represents the model for a geometric phase delay that is phase and amplitude matched to the first peak of the data. (right) The same VPM was also tested at 3.15 mm. In this case, no phase or amplitude adjustment was done. In this case, the phase more closely matches that of the geometrical case. In each case, the bandwidth is ∼10%

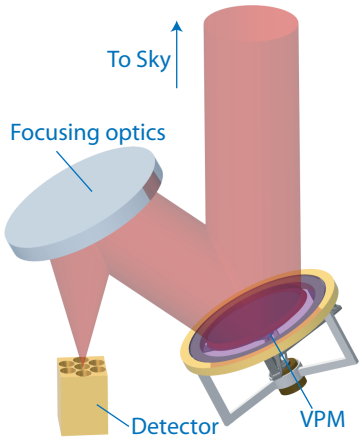

Figure 3. The optical path includes a VPM as the first component in the system.

where appropriate below, work on reflective HWPs will be included since it gives valuable insight into the electromagnetics of the grid-mirror system.

6.1. Beam Walkoff

For the mirror-grid system, the two polarizations are displaced relative to one another a distance $x = 2d \sin\phi$. This quantity, x, is the "walkoff" and for the VPM varies with the modulation variable, d. This leads to a potential synchronous pickup; however this can be mitigated in two ways. First, this effect can be reduced by choosing small incidence angles. Second, if the VPM is located at a pupil in the optical system, then a parallel shifting of the output beams will not change the relative angle between the beams in the two orthogonal polarizations.

6.2. Variable Beam Truncation

At non-normal incidence, the back optical surface of the VPM will be vignetted by the frame of the front optical surface. The amount of vignetting will depend on grid-mirror separation and so will vary with the modulation. An adequate edge taper will ameliorate this problem. In addition, the symmetry of the concept can help as well. The beam truncation is such that it will affect the Stokes U polarization state. Variations in the light reflected off of the back surface of the VPM will show up in each of the (polarized) detectors as common-mode variations and can be differentiated from the antisymmetric variation of the modulated Q polarization state. Of course, this is only strictly true for the central ray of the system and the effect of beam truncation will vary across the array.

6.3. Grid Emissivity and Resonances from Trapped Modes.

The emissivity of the grid wires will combine with polarization leakage to cause emission and absorption that will be a function of the grid-mirror separation. Cooling the VPM to 2.73 K will mitigate this risk, but this will impact spacecraft design and will certainly require development effort for cryogenic VPMs. Again, the symmetry of the system helps here as well. Emission and absorption will affect the Stokes U value, but will appear as common-mode in the two orthogonal detectors. The full effect of this will need to be studied in more detail.

An additional effect of imperfect polarization isolation is that radiation can become trapped between the grid and the mirror. This effect has been observed in such grid-mirror systems (for an example, see Houde[7]). This effect is also thought to be responsible for the complex interferometer behavior in Manabe[10]. For broadband operation, this effect is diluted significantly. In addition, optimizing the wire size for the wavelength range will also help mitigate this problem.

6.4. Dependence on Grid Properties

Extensive literature has been devoted to the electromagnetic modeling of polarizing grids (see Houde [7] and references therein). In the limit where the wavelength is much larger than the wire diameter, the polarizing grid approaches ideal behavior with high isolation between the two orthogonal polarizations. In this case, the phase delay introduced by a VPM is proportional to the path difference between the two polarizations as stated above. As this assumption is violated, the phase delay acquires a second contribution due to a reactive component that has a nontrivial dependence on grid-mirror separation. This has been noted by Krejny[12]; however the effect requires more study.

7. Technology Development

7.1. Parallel Transport Mechanism

In order to ensure that the two beams recombine at the same angle, and that the phase difference is well-defined, it is essential that the transport mechanism used to control this mechanism maintain parallelism. This problem is similar to that encountered in Fabry-Perot systems, and similar tolerances apply. One way of constraining parallelism is to employ a system of 3 motors with feedback to control the parallelism [19]. Another is to mechanically constrain all but one degree of freedom and control the position with a single feedback loop [20]. The latter has been implemented in the Hertz/VPM submillimeter polarimeter [21]. Work on a similar system for an Inflation Probe modulator is underway, but not yet complete.

The Hertz/VPM devices used piezoelectric motors for motion. The COFE modulator used a linear coil-based motor. In the latter case, the transport stage was driven at resonance to ease control for fast modulation. The feedback can be controlled with a variety of sensors including capacitive devices as well as optical encoders.

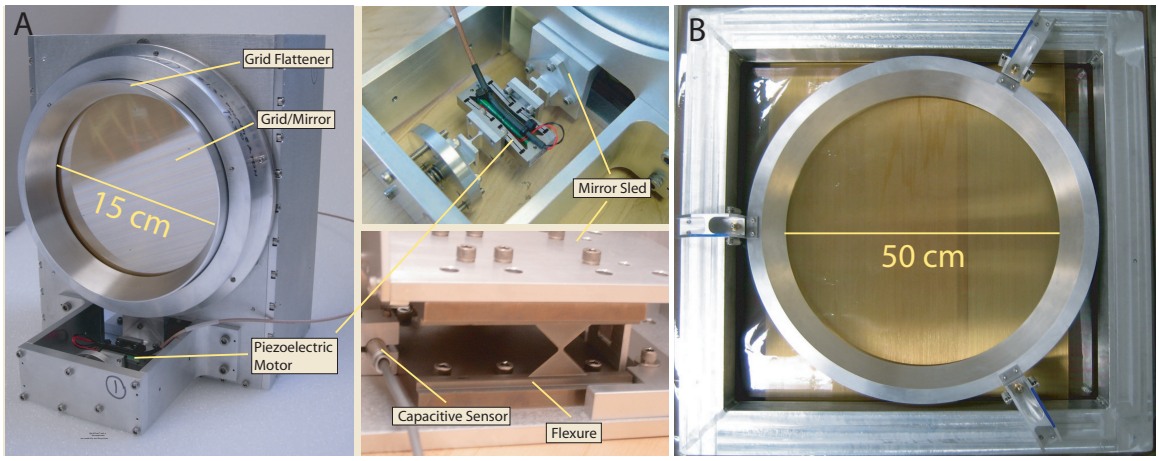

Figure 4. The VPM used in the Hertz/VPM experiment is shown in (A). A 50 cm diameter grid with grid flattener is shown.

7.2. Grid Construction

In order to achieve modulation at the primary aperture for Inflation Probe, VPMs will have to exceed 50 cm in diameter. Grids are typically made by wrapping wire over the grid frame [22]. An alternative technique is based on work by Novak[23] and involves wrapping wires onto a cylindrical mandrel and then transferring them to a grid frame. The latter technique has been used to construct a 50 cm diameter polarizing grid with 63.5 μm wires on a 200 μm pitch (See Fig. 4). The resonant frequency of the wires was greater than 128 Hz, much larger than the ∼few Hz modulation frequency. Using the grid flattener, a planarity of the grid surface that was below 50 μm was achieved.

Because the phase definition is of utmost importance with a VPM, the wire surface must be flat to a small fraction of a wavelength. Grid flatteners have been used in both the Hertz/VPM VPMs [21] and in the prototype CMB wire grid [24].

8. Summary of VPM Advantages/Disadvantages

Advantages

- VPMs are a practical solution for modulation at the front of the optical system because they can be made larger than dielectric HWPs and operate in translation rather than rotation.
- The interferometric modulation scheme provides potential for multi-band, broad-band, or spectropolarimetric use.
- Primary modulation can be done in polarization rather than photometric scanning.
- The translational flexure is frictionless and can be engineered for long, reliable operation in space.
- Systematic control has the potential to be high, due to the capability of "hiding" systematics (e.g. those due to differential loss) in the unmeasured linear Stokes parameter.
- The sensitivity to Stokes V can provide an additional calibration tool.
- "Leakage" term is V rather than U, and therefore VPM may provide good control of (E, B) mixing systematic.
- No transmissive dielectrics are required, thereby mitigating dielectric loss, cavity formation, and large cosmic ray cross section.

Disadvantages

- The VPM is not as tested as the HWP (VPM is at TRL 3).
- Measurement of only one linear Stokes parameter at a time requires spacecraft rotation or cross-calibration with another optical system for complete polarization determination.
- The use of VPMs for front-end modulation would be problematic for high angular resolution experiments. It would be practically limited to lower multipole, large scale B-mode searches.
- Since only one linear Stokes parameter is measured at a time, the modulation efficiency is dependent on the angle of the grid wires to the incident polarization. This introduces an integration time penalty.
- The VPM is most likely limited to systems with low enough 1/f such that the practical modulation frequencies of ∼1-10 Hz would be useful. (This would include bolometer-based systems, but perhaps not many coherent detectors).

9. Path to TRL 5

- The flexure concept needs to be adapted for the large aperture VPM. (1.5 Person Years + 50k)
- The continuous ∼few Hz modulation/demodulation functionality needs to be tested (1.5 Person Years + 50k)
- The flexure and grid need to be adapted for cryogenic use. (1.5 Person Years + 150k)
- Cryogenic microwave testing must be done. (1.0 Person Years + 100k)
- System demonstration leading to astrophysical data product on ground-based or suborbital platform.

References

[1] Martin D and Puplett E 1970 *Infrared Physics* **10** 105–109
[2] Mather J C, Fixsen D J and Shafer R A 1993 *Proc. SPIE Vol. 2019, p. 168-179, Infrared Spaceborne Remote Sensing, Marija S. Scholl; Ed.* (*Presented at the Society of Photo-Optical Instrumentation Engineers (SPIE) Conference* vol 2019) ed Scholl M S pp 168–179
[3] Martin D 1974 *Infrared and Millimeter Waves* vol 6 ed Button J (Academic Press)
[4] Battistelli E, DePetris M, Lamagna L, Maoli R, Melchiorri F, Palladino E and Savini G 2002 *astro-ph/0209180v1*
[5] Catalano A, Conversi L, de Gregori S, de Petris M, Lamagna L, Maoli R, Savini G, Battistelli E S and Orlando A *New Astronomy*
[6] Howard J, Peebles W and NC Luhmann J 1986 *IJIMW* **7** 1591–1603
[7] Houde M, Akeson R L, Carlstrom J E, Lamb J W, Schleuning D A and Woody D P *PASP*
[8] Akeson R L, Carlstrom J E, Phillips J A and Woody D P 1996 *ApJL* **456** L45+
[9] Erickson N 1978 *IEEE MTT-S Intl. Microwave Symposium Digest* 438–439
[10] Manabe T, Inatani J, Murk A, Wylde R J, Seta M and Martin D H 2003 *IEEE Transactions on Microwave Theory and Techniques* **51** 1696–1704
[11] Erickson N 1987 *IJIMW* **8** 1015–1025
[12] Krejny M, Chuss D, Drouet d'Aubigny C, Golish D, Houde M, Hui H, Kulesa C, Loewenstein R F, Moseley S H, Novak G, Voellmer G, Walker C and Wollack E 2008 *Applied Optics* **in press** (*Preprint* 0803.3759)
[13] Chuss D T, Wollack E J, Moseley S H and Novak G 2006 *Applied Optics* **45** 5107–5117
[14] Lubin P 2005 *Private Communication*
[15] Leonardi R, Williams B, Bersanelli M, Ferreira I, Lubin P M, Meinhold P R, O'Neill H, Stebor N C, Villa F, Villela T and Wuensche C A 2006 *New Astronomy Review* **50** 977–983
[16] Shinnaga H, Tsuboi M and Kasuga T 1999 *PASJ* **51** 175–184
[17] Siringo G, Kreysa E, Reichertz L A and Menten K M 2004 *Astronomy and Astrophysics* **422** 751–760
[18] Chuss D and Wollack E 2008 *In preparation*
[19] Staguhn J G, Benford D J, Pajot F, Ames T, Allen C A, Chervenak J A, Lefranc S, Maher S, Moseley Jr S H, Phillips T, Rioux C G, Shafer R A and Voellmer G M 2004 *Millimeter and Submillimeter Detectors for Astronomy II. Edited by Jonas Zmuidzinas, Wayne S. Holland and Stafford Withington Proceedings of the SPIE, Volume 5498, pp. 438-445 (2004).* (*Presented at the Society of Photo-Optical Instrumentation Engineers (SPIE) Conference* vol 5498) ed Bradford C M, Ade P A R, Aguirre J E, Bock J J, Dragovan

M, Duband L, Earle L, Glenn J, Matsuhara H, Naylor B J, Nguyen H T, Yun M and Zmuidzinas J pp 438–445
[20] Bradford C M, Stacey G J, Swain M R, Nikola T, Bolatto A D, Jackson J M, Savage M L, Davidson J A and Ade P A R 2002 *Applied Optics* **41** 2561–2574 (*Preprint* `arXiv:astro-ph/0205159`)
[21] Voellmer G M, Chuss D T, Jackson M, Krejny M, Moseley S H, Novak G and Wollack E J 2006 *Optomechanical Technologies for Astronomy. Edited by Atad-Ettedgui, Eli; Antebi, Joseph; Lemke, Dietrich. Proceedings of the SPIE, Volume 6273, pp. 62733P (2006).* (*Presented at the Society of Photo-Optical Instrumentation Engineers (SPIE) Conference* vol 6273)
[22] Lahtinen J and Halilikainen M 1999 *IJIMW* **20** 3
[23] Novak G, Sundwall J L and Pernic R J 1989 *Applied Optics* **28** 3425–3427
[24] Voellmer G M, Bennett C L, Chuss D T, Eimer J, Hui H, Moseley S H, Novak G, Wollack E J and Zeng L 2008 *in preparation* Presented at the Society of Photo-Optical Instrumentation Engineers (SPIE) Conference